



Universidad de Cantabria

Facultad de Ciencias

**ON LIGHT SCATTERING BY NANOPARTICLES WITH
CONVENTIONAL AND NON-CONVENTIONAL
OPTICAL PROPERTIES**

PH.D. THESIS

Braulio García-Cámara

Santander, July 2010

Part III

Study of Light Scattering by a Nanoparticle Above a Substrate

8

Interaction of Nanoparticles with Substrates: Effects on the Dipolar Behavior of the Particles.

*"A ver qué puedes hacer
Poner de tu parte para ver"
—El canto del loco, grupo musical español*

8.1. Introduction

After several chapters dedicated to the study of the scattering properties of nanoparticles with unconventional optical properties, this one is devoted to a more realistic system, reproducing experimental geometries. Along this thesis, we have pointed out the existence of many applications in several fields, from biology [17] to new energy technologies [19], based on plasmonic properties of metallic nanoparticles. The excitation of localized surface plasmon resonances (LSPRs), producing important enhancements of the scattered and absorbed electromagnetic fields, is the main physical feature on which those applications are based. Many of the experimental setups of the aforementioned applications, nanoparticles must be on or close to a substrate. The presence of the substrate underneath and the interactions between both elements, modifies the scattering properties of the nanoparticles

[102]. These modifications can be analyzed providing information about the properties and the profile of the surface. Some works have been devoted to this kind of experiments using nanoparticles as probe nanoantennas for monitoring surfaces [63, 79] or for a new generation of near-field optical microscopes [67]. The main advantage of these techniques is that they are able to obtain information in the near-field range by measuring light scattering in the far-field which is much easier to detect than the near-field. New applications and techniques based on nanoparticles have shown the importance of a detailed knowledge of the local field distribution [106].

When a metallic nanoparticle is isolated or far from any substrate, the dipolar character is well defined. The angular distribution of the scattered electric field follows the typical "eight-shape" with a charge concentration in the equator of the nanoparticle if the incident polarization is parallel to the scattering plane [108]. As the nanoparticle approaches a substrate, the local electric field distribution deviates from the dipolar shape due to charge oscillation modes produced by the influence of the surface underneath. In this chapter, we have analyzed the interactions and the modes induced in the nanoparticle by the presence of the surface in its surroundings using as an indicator the distribution of the scattered electric field on the surface of the nanoparticle and more specifically, the position of the maximum of the distribution. Following the usual materials used in experiments, the particles have been considered made of silver or gold and the substrates are either dielectric or metallic, in particular glass and gold respectively.

Three dimensional ($3D$) simulations for an isolated particle, clusters or particles above substrates are common nowadays [68, 71, 142]. However, for regular geometries and for certain types of illumination (commonly found in experiments), $2D$ simulations are more than enough to understand the physics of the problem [102]. We have dedicated one section to show that the differences between $3D$ and $2D$ calculations lie in the values and not in the physics. This result allow us to use $2D$ geometries for the rest of the chapter reducing the complexity of the calculations.

8.2. Comparison between $2D$ and $3D$ Geometries

As it was mentioned, some $3D$ problems can be interpreted correctly using a $2D$ geometry. To demonstrate this, we have calculated and compared the distribution of the modulus of the electric field on the surface of an isolated sphere ($3D$) and an isolated cylinder ($2D$). In both cases, the object is illuminated by a plane wave. In order to compare the results for both

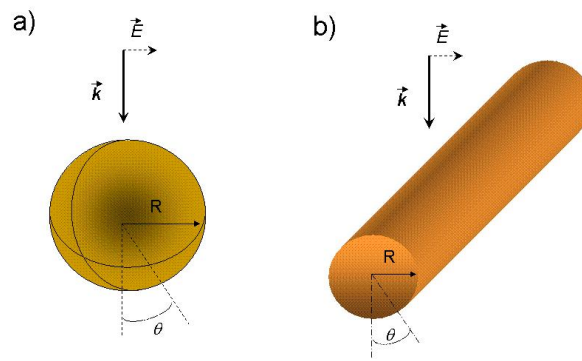


Figure 8.1: Scheme of the considered geometries.

cases, the beam illuminating the cylinder must have a propagation direction perpendicular to its main axis and linearly polarized with the electric field vector also perpendicular to the longest axis (see Figure 8.1). This polarization is the one able to excite surface plasmon resonances in infinitely long metallic cylinders. On the contrary, due to the sphere's symmetry, the illumination conditions are much less restrictive.

The calculations are performed using a finite element method (FEM) and by means of our own modification of the programs contained in [13]. In Figure 8.2 the angular distribution of the local electric field on the surface of (a) a cylinder and (b) a sphere are plotted. In both cases the particle is made of silver with a radius $R = 25nm$. Three values for the incident wavelength are considered; below, on and above the plasmon resonance which appears at $\lambda = 348nm$ and $\lambda = 364nm$ for a silver cylinder and a silver sphere of the considered size, respectively. Also, a larger particle size is considered for one of the wavelengths in order to observe the influence of the size.

For an isolated silver cylinder out of resonance (green triangles), the local electric field has the typical "eight-shape" dipolar distribution for a very small particle in the near field regime [108]. An increment of the particle size (blue diamonds) makes the quadrupolar mode more important and by this disturbing the dipolar shape and shifting the maxima of the local electric field towards the forward direction ($\theta = 0^\circ$). If the incident wavelength is resonant for the particle (red circles), the values for the electromagnetic fields around it increase while the distribution remains quite similar to the dipolar behavior. In this case, the dipolar shape is slightly modified because for a silver cylinder of $R = 25nm$ and for $\lambda_{inc} = 348nm$ the dipolar and the quadrupolar resonances overlap (see Figure 1 of reference [102]). This coincidence results in the shift of the maximum of $|E|$ towards the forward direction. The angular distribution, however, is radically different for incident wavelengths below the resonant one. For $\lambda = 325nm$, the refractive index of silver tends to lose its metallic behavior

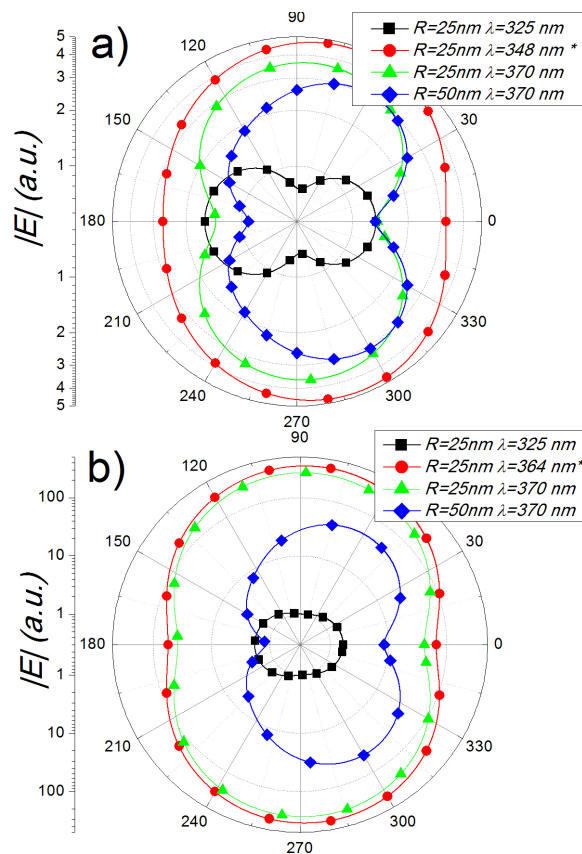


Figure 8.2: Angular distribution of the modulus of the electric field on the surface of (a) an isolated silver cylinder and (b) an isolated silver sphere for three different wavelengths around the plasmon resonance and two different particle sizes. * means that the wavelength correspond with the plasmon resonance for that geometry.

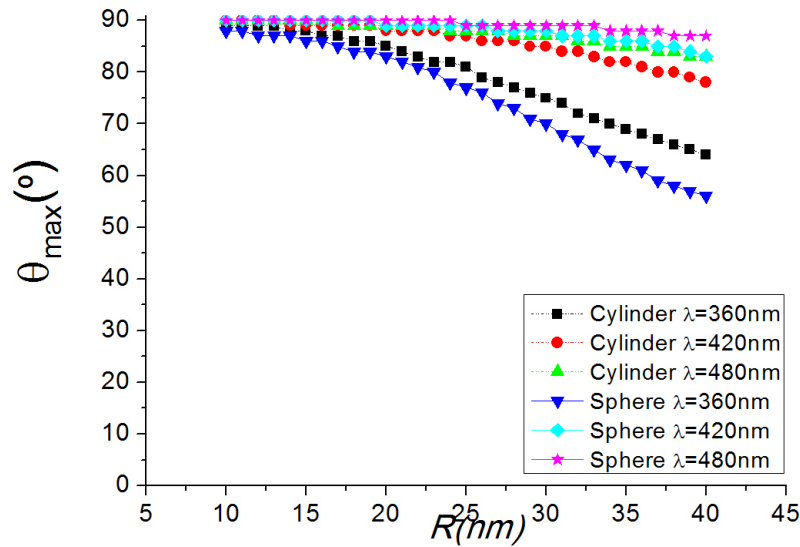


Figure 8.3: Angular position of the maximum of the local electric field (θ_{max}) around an isolated silver sphere or an isolated cylinder as a function of the radius and for several incident wavelengths.

and becomes dielectric-like, since for this wavelength, the permittivity becomes positive. Now, comparing the qualitative behavior of the cylinder and the sphere, we can conclude that the angular distribution is quite similar for both geometries. The main difference, apart from the values, appears for the resonant wavelength. While for the cylinder, the dipolar and quadrupolar resonances overlap, this does not occur for the sphere. The maxima for the sphere point towards the 90° direction while the ones of the cylinder point towards the forward direction.

In this figure, it can be observed that the angle at which the local electric field reaches a maximum (θ_{max}) is quite sensitive to any change in the field distribution, in particular to any effect that produce a departure from the pure dipolar behavior. Using it as a fast indicator of the distribution of the field, a qualitative comparison can be performed. For this task, we have plotted θ_{max} versus the particle size in Figure 8.3 and as a function of the incident wavelength in Figure 8.4.

In Figure 8.3, the angle at which the local electric field is maximum (θ_{max}) is shown as a function of the particle size either for a silver cylinder or a silver sphere. Three different incident wavelengths are considered. These incident values: 360nm , 420nm and 480nm correspond to resonant wavelengths for silver spheres of sizes $R = 20$, 65 and 82nm , respec-

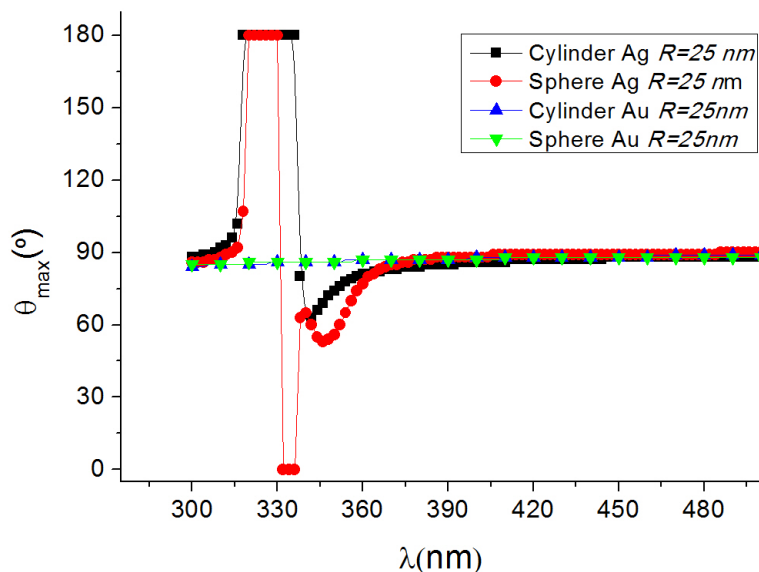


Figure 8.4: Angular position of the maximum of the local electric field (θ_{max}) around an isolated silver sphere (red circles) or an isolated cylinder (black squares) with size $R = 25nm$ as a function of the incident wavelength. The same calculations for gold are also included.

tively. For small sizes and for each incident λ , the angular distribution shows a pronounced dipolar behavior and as a consequence, θ_{max} tends to 90° . As the particle, either the sphere or the cylinder grows, orders higher than the dipolar one disturb the dipolar behavior, shifting θ_{max} to lower values. This evolution is smaller for larger wavelengths. We attribute this to the reinforcement of the dipolar behavior as the incident wavelength differs from the resonant regions, as is observed in Figure 8.4.

The curves plotted in Figure 8.4 correspond to the evolution of θ_{max} as a function of the incident wavelength for a cylinder and a sphere made of silver or gold and $R = 25nm$. As it can be seen, for incident wavelengths larger than $\sim 360nm$ the curves saturates towards 90° which means that every particle radiates as an electric dipole. This behavior is produced by the well-defined metallic character of silver and gold in this range. Also, the ratio (R/λ) reinforces the validity of the electrostatic approximation independently from the geometry and the optical constants of the particle. For lower values of λ , the evolution is much more complex due to the increment of the ratio (R/λ) but also due to the particularities of the evolution of the refractive index of silver [60]. The dielectric constant of silver presents an intricate evolution in the range $\lambda \in [300, 360]nm$. in part due to the interband transitions. It must remarked that silver changes from a metallic to a dielectric behavior (that is, the real part

of ϵ changes its sign) around $325nm$ and its refractive index reaches the values -1 and -2 at $\lambda = 338nm$ and $\lambda = 355nm$, respectively. These last two values correspond to the Fröhlich resonances of a infinitely thin cylinder and a point-like sphere, respectively. Two interesting features can be observed related with these important values of the refractive index. First, θ_{max} reaches a minimum around the position of the resonant value of the refractive index. The position of this minimum depends on the resonant condition and then on the geometry and the size of the particle (for $R = 25nm$ the resonant wavelengths for a cylinder and a sphere are 350 and $358nm$ respectively). Furthermore, an abrupt change appears when the the particle's refractive index matches the index of the surrounding medium. For a silver particle embedded in vacuum, this pseudo-matching is found for $\lambda \simeq 338nm$ for which $|Re(\epsilon_{Ag})| = 1$. This effect has been analyzed in more detail in Figure 8.5 where θ_{max} has been plotted versus λ for a silver cylinder with two different sizes and embedded in air and in a medium with higher density ($n = 1.5$). In this figure, we can observed that as the refractive index of the surrounding medium changes from $n = 1$ to $n = 1.5$, the spectral position of θ_{max} (from the top-backward to the mid-forward part) also changes from $\sim 338nm$ to $\sim 360nm$, respectively. For this last value, the dielectric constant of silver reaches the value $|Re(\epsilon_{Ag})| \simeq 2.28$ which is close to the dielectric constant of the denser medium. The curve for a smaller size is also shown in Figure 8.5 to demonstrate the independence of this effect with respect to the particle size. It can also be demonstrated that these results are similar for an spherical geometry.

While the last explanations are focused on the silver particles, the behavior of the particles made of gold is quite different in the range $\lambda \in [300, 360]nm$. (see Figure 8.4). The evolution of the dielectric constant of gold is more stable in this range in such a way that the real part is always negative (the zero crossing of $Re(\epsilon)$ occurs at a wavelength lower than $300nm$.) and it does not reach the values -1 or -2 . Because of that, gold particles show a dipole-like behavior along the whole range of wavelengths considered. This means that θ_{max} stays close to 90° for both gold geometries and at every λ .

At the view of the results, we can conclude that, under the considered conditions of our study, the distributions of the local electric field, the localization of its maximum and other interesting effects (pseudo-matching, spectral localizations of the quadrupolar effects and resonances), there is a qualitative parallelism between a $2D$ (cylindrical) and a $3D$ (spherical) geometries. Therefore, maintaining the conditions of illumination (spectral range and polarization) and size, we shall consider in what follows a $2D$ geometry instead of a $3D$ one, i.e. a metallic cylinder above a flat substrate.

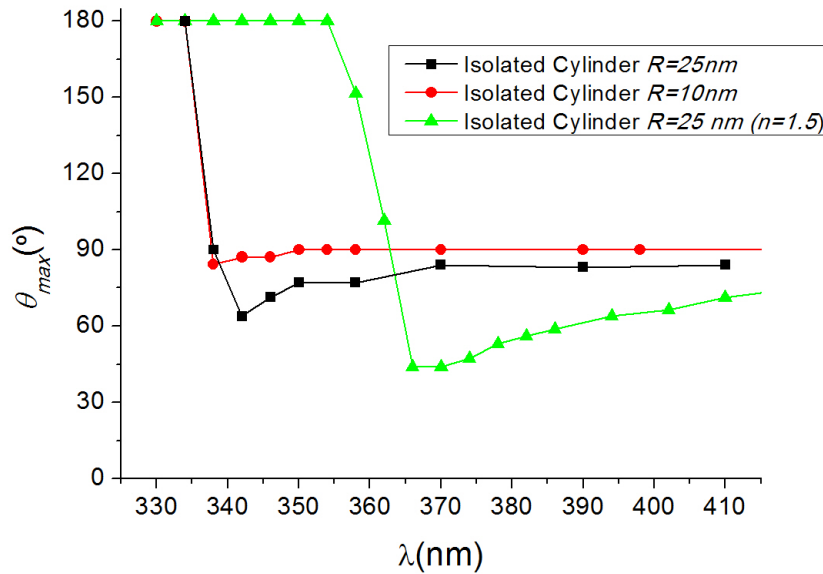


Figure 8.5: Angular position of the maximum of the local electric field (θ_{max}) around an isolated cylinder made of silver for two different sizes and for a case in which the surrounding medium is denser ($n = 1.5$) than air.

8.3. Particle Above a Dielectric Substrate

In this section we will study the influence of the presence of a substrate underneath a metallic cylinder on the local field distribution of it. The cylinder is considered with a circular cross-section of radius R and made of a noble metal (silver or gold) and it is located above a semi-infinite surface at a distance d (see Figure 8.6). The substrate has been considered made of either dielectric or metal (as it will be explained in the next section) because these are typical situations in experimental set-ups [125]. The system is also illuminated with a plane wave whose propagation direction is perpendicular to both the cylinder axis and the substrate and linearly polarized with the incident electric field also perpendicular to the cylinder axis. The angle at which the local electric field reaches a maximum is calculated following the same convention as in the isolated case, as is shown in Figure 8.6.

Taking into consideration the previous results about the differences between isolated spherical ($3D$) and cylindrical ($2D$) geometries, we now assume that the local electromagnetics involved in the scattering problem of a cylinder above a flat substrate is representative, to some extent, of an spherical particle above a similar substrate. To ensure that both situations are qualitatively equivalent, both problems should have the same geometrical section

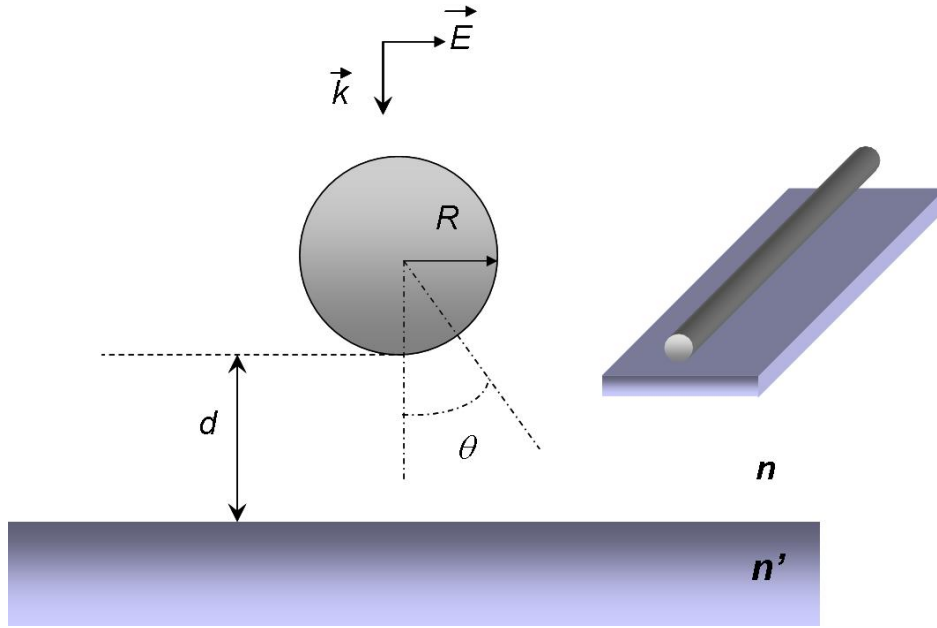


Figure 8.6: Cross section of the considered geometry consisting of a metallic cylinder embedded in a medium with refractive index n and above a flat substrate with a refractive index n' at a distance d . The system is illuminated by a plane wave linearly polarized. As inset we have include the complete geometry whose cross section is explained in detail.

and optical parameters. Also the illumination direction and the scattering plane must be perpendicular to the main axis of the cylinder and, more important, the polarization has to be in such a way that the incident electric field is also normal to the cylinder axis, as it is shown in Figure 8.6. Under these conditions, the results we will show for a cylindrical geometry could be extended for a spherical one, in other words, the results for the $2D$ geometry can be generalized to a $3D$ geometry. This extension cannot be applied for other profiles, in particular for particles with irregular shapes that present very particular field distributions as it has been shown in [106].

The first step for the analysis of the influence of the substrate is shown in Figure 8.7. In it, we show the spectral evolution of the angular position of the maximum of the local field (θ_{max}) for a cylinder made of silver (optical constants from [60]) and radius $R = 25nm$ for several distances (d) between the particle and the substrate made of glass ($n' = 1.5$). The case of the isolated cylinder is also included in order to show the tendency of the other curves towards this curve as d increases. The drastic change observed in the position of θ_{max} at short wavelengths corresponds, as it was mentioned in the previous section, to the pseudo-matching of the dielectric constant of the cylinder at this wavelength and the surrounding medium (in this case $Re(\epsilon_{Ag}) = \epsilon_{surround} = 1$). For the isolated cylinder, after this flip,

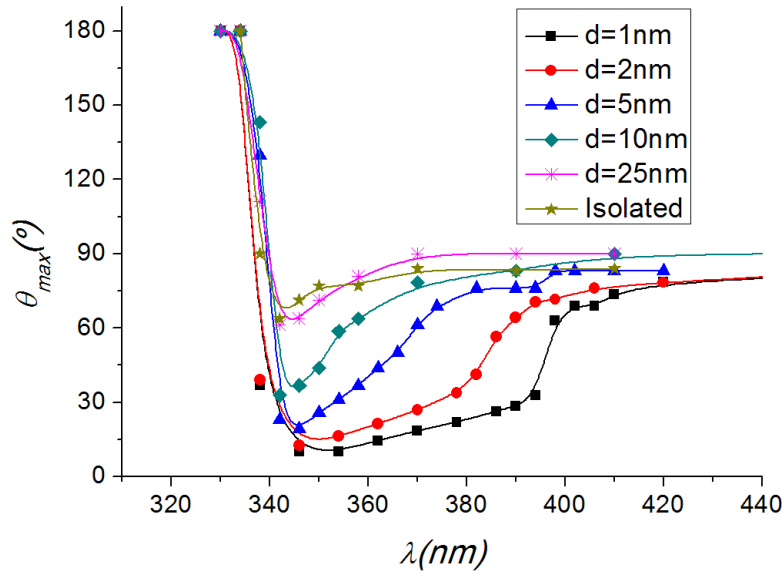


Figure 8.7: Angular position of the maximum of the surface electric field (θ_{max}) of a silver cylinder ($R = 25nm$) above a flat substrate ($n' = 1.5$) as a function of the incident wavelength and for several values of the gap between the cylinder and substrate. Also the case of the isolated cylinder is included for comparison.

θ_{max} tends to the dipolar behavior (the maximum located on the equator of the cylinder) reaching a minimum around the incident wavelength at which the surface plasmon resonance is excited. If, now, we approach a flat surface to the cylinder, the maximum of the local electric field stays at the bottom part of the particle, that is the part facing the substrate, for a certain spectral range. This range is longer as the gap between the cylinder and the substrate below it decreases. Then, the interaction with the substrate pushes the cylinder to the dipolar behavior ($\theta_{max} \rightarrow 90^\circ$) for larger wavelengths. In other words, the presence of the substrate shifts the dipolar behavior of the metallic cylinder to the red part of the spectrum. This effect is in agreement with the effect of the substrate on the surface plasmon resonance as it was studied in [102].

The influence of the substrate and in particular, the effect of the concentration of the electric field in the gap between the cylinder and the flat surface is quite interesting and could have several applications in surface lithography at the nanoscale range [145]. This can be observed in Figure 8.8 where we show the polar distribution of the electric field around a silver cylinder with $R = 25nm$ at a distance $d = 1nm$ above a glass substrate ($n' = 1.5$) and for several incident wavelengths, one of these being resonant for the geometry. As can

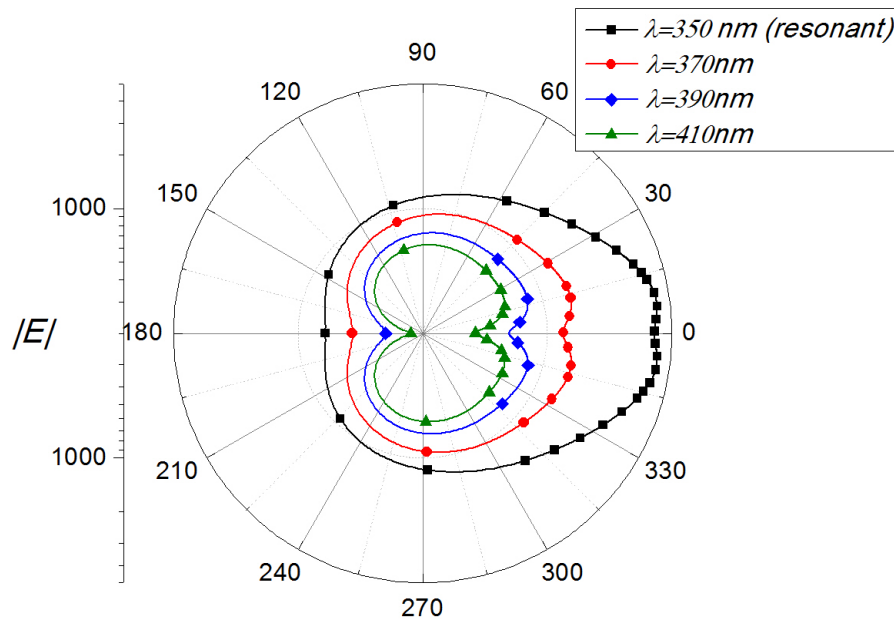


Figure 8.8: Scattering diagram of a silver cylinder ($R = 25nm$) above a dielectric substrate ($n'=1.5$) with a gap between them of $d = 1nm$ and for several incident wavelengths.

be seen, the presence of the flat surface disturbs the surface electric field distribution shifting the maximum towards the forward direction (the part of the cylinder facing the substrate), as it was mentioned. When the incident wavelength is resonant (black squares), the scattered intensity increases considerably, as is expected, showing an unusual shape with very high values on the side facing the substrate and an interesting double-peak structure. As the incident wavelength increases, that is the wavelength tends to the red, the polar distribution runs to the typical "eight-shape" of the dipolar behavior for the considered incident polarization.

As in the case of the localized surface plasmon resonances, the red-shift of the wavelength at which the cylinder acquires the dipole-like behavior is also dependent on the particle size. In Figure 8.9, θ_{max} is plotted versus λ for two sizes of the metallic cylinder ($R = 10nm$ and $R = 25nm$) and for two values of the gap-distance: (a) $d = 1nm$ and (b) $d = 5nm$. It can be seen that the local electric field distribution depends on the particle size. The spectral range in which the maximum of the surface electric field is facing the substrate gets narrower as R decreases. It could get even narrower if the distance to the substrate was increased (Figure 8.9(b)).

In some experimental situations [64, 96], the surrounding medium must be denser than the substrate. The effect of this change in the refractive indexes produces a blue-shift of the surface plasmon resonance [102] due to a reinforcement of the electric charge oscillation

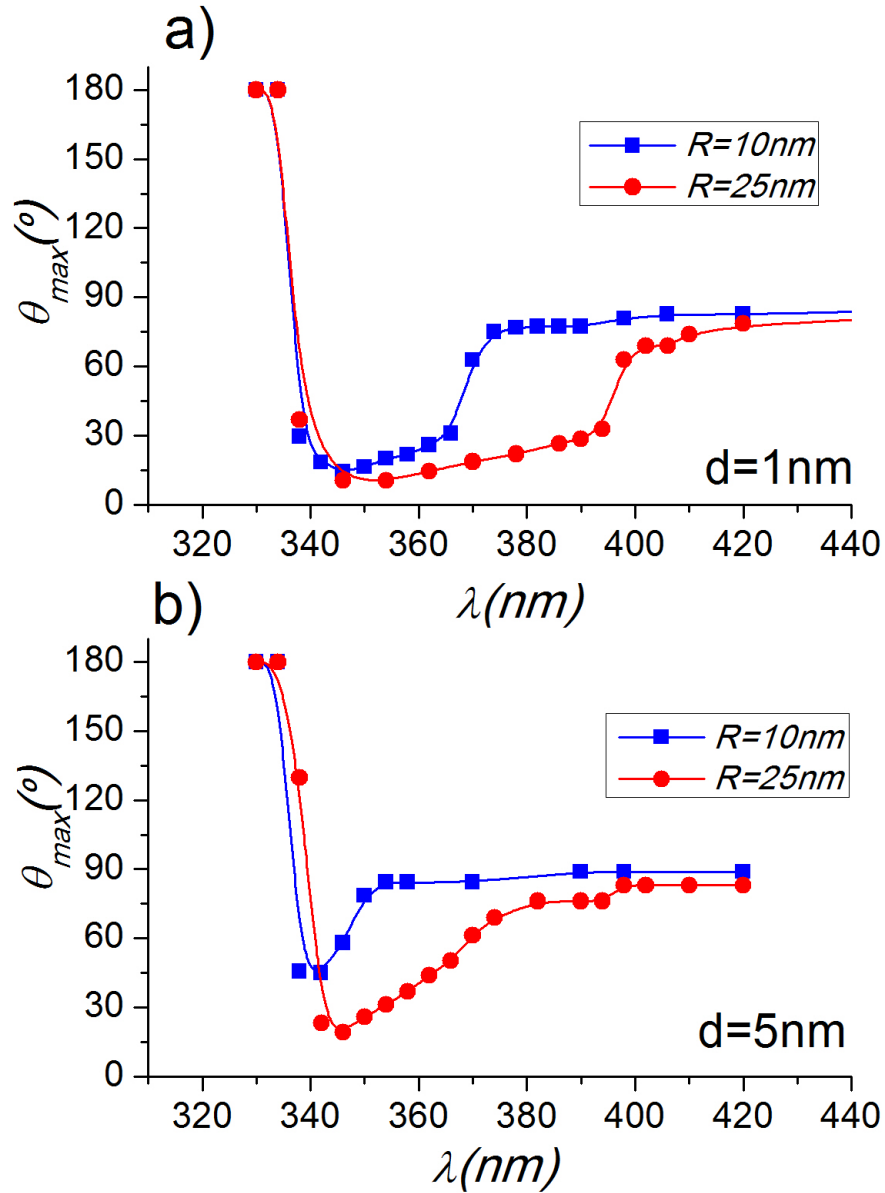


Figure 8.9: Angular position of the maximum of the local electric field (θ_{max}) around a silver cylinder of two different sizes above a dielectric substrate ($n' = 1.5$) at a distance: (a) 1nm and (b) 5nm as a function of the incident wavelength.

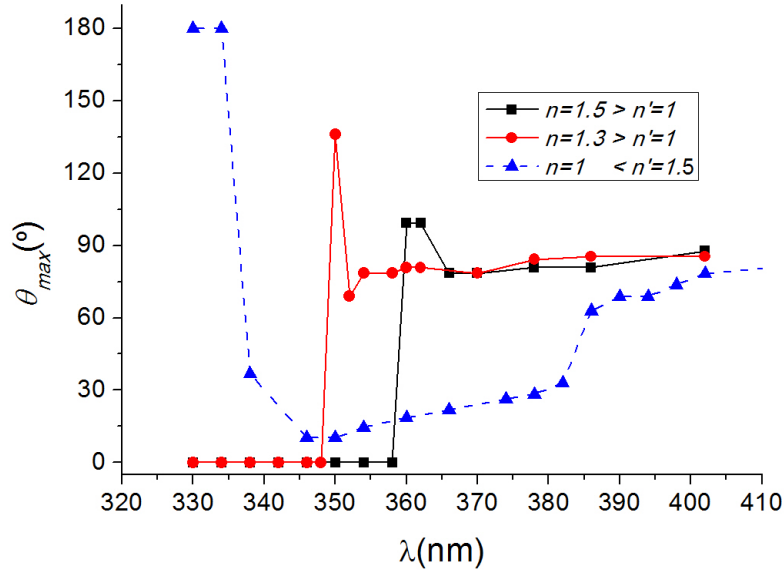


Figure 8.10: Angular position of the maximum of the local electric field (θ_{max}) around a silver cylinder of two different sizes above a flat substrate at a distance $d = 1nm$ as a function of the incident wavelength and for different combinations of the refractive indexes of the surrounding medium and the substrate.

in the particle. When $n > n'$ the sign of the reflection coefficient of the interface does not change and the reflected field produces a constructive superposition. The first idea is that if the surface plasmon resonance is blue-shifted, the wavelength at which the cylinder reaches the dipolar behavior must be also blue-shifted, as it was red-shifted in the previous case. To observed this, in Figure 8.10 we have plotted θ_{max} for a cylinder of $R = 25nm$ at a distance $d = 1nm$ with an air substrate ($n'=1$) and a denser surrounding medium: $n = 1.5$ (■) and $n = 1.3$ (●). For comparison, we have also included the previous case with $n = 1$ and $n' = 1.5$ (▲).

As can be seen, the previous idea is right. When $n > n'$, the dipole-like behavior ($\theta_{max} \rightarrow 90^\circ$) appears for shorter incident wavelengths than for the case $n < n'$. In addition, this behavior is preceded by a transition region whose peak corresponds to the incident wavelength at which the dielectric constant of the particle ($|Re(\epsilon_{Ag})|$) matches that of the surrounding medium, that is the pseudo-matching that was mentioned in the previous section.

Until now we have considered always a silver cylinder. However, we can consider a cylinder made of gold in order to complete this study. Figure 8.11 summarizes the main

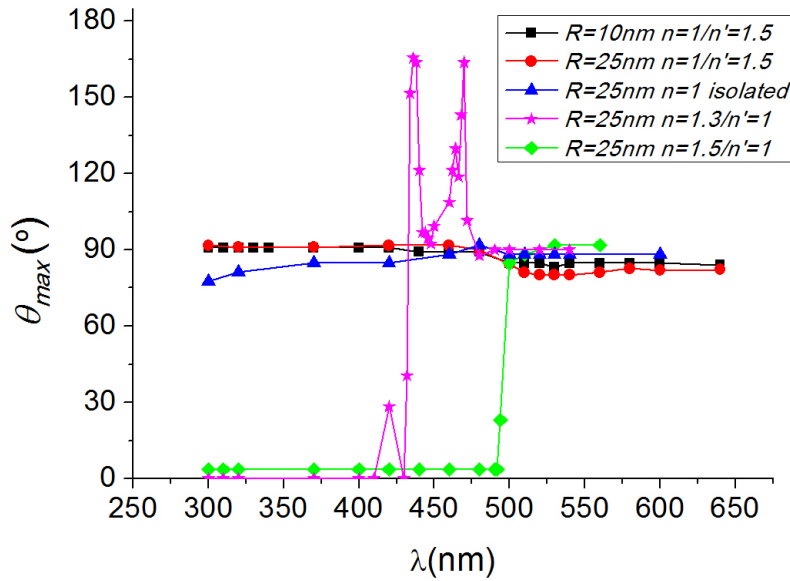


Figure 8.11: Angular position of the maximum of the local electric field (θ_{max}) around a gold cylinder above a flat substrate at a distance $d = 1nm$ as a function of the incident wavelength for two different particle sizes and for different combinations of the refractive indexes of the surrounding medium and the substrate.

results concerning the gold cylinder. Triangles (\blacktriangle) correspond to the isolated case for a $R = 25nm$. The case of the gold cylinder embedded in vacuum ($n = 1$) and above a glass substrate ($n'=1.5$), that is the $n < n'$ case, is represented for sizes of $R = 10nm$ (\blacksquare) and $R = 25nm$ (\bullet). For these cases the evolution of θ_{max} is quite regular and it is almost equal to 90° for the whole spectral range. This behavior is directly related to the optical properties of gold [60] and their evolution with λ in this range. In the considered spectral range, gold has a pronounced metallic signature ($\epsilon \ll 0$) with no matching with the surrounding medium. However, if the surrounding medium is denser (Figure 8.11, solid diamonds(\blacklozenge) and stars(\star)) the behavior is more complex. Two different conducts can be observed: below and above the transition regions where $|Re(\epsilon_{Au})|$ matches the dielectric constant of the surrounding medium around $\lambda = 440nm$ for the case($n = 1.3, n' = 1$) and $\lambda = 494nm$ for ($n = 1.5, n' = 1$).

Below these wavelengths, the maximum of the surface field is stable at the part of the cylinder facing the interface while for larger wavelengths it tends to the equator of the particle (dipolar behavior). When the refractive index of the cylinder and the surrounding medium match, that is in the transition region, the local electric field, as happens also for silver, is uniformly distributed around the cylinder reaching very high values ($10^5 - 10^6$ times the

incident field). The sharp peaks that appear for the case of $n > n'$ in this region for silver and gold (Figures 8.10 and 8.11, respectively) are produced by the non-monotonic dependence of the refractive index of these materials with the incident wavelength within the pseudo-matching interval. Therefore, it can be observed that the angular position of the maximum (θ_{max}) oscillates before reaching the dipolar behavior.

As an example illustrating the different behaviors described above, in Figure 8.12, the spatial distribution of the electric field around a gold cylinder of $R = 25nm$ embedded in glass ($n = 1.5$) and at a distance ($d = 1nm$) above an interface with vacuum ($n' = 1$) is calculated using a FEM (finite-element method) tool for three representative incident wavelengths: well below ($\lambda = 420nm$), well above ($\lambda = 560nm$) and inside the transition zone ($\lambda = 496nm$). Every feature described before can be observed in this plot and similar figures can be obtained in the transition area associated to a silver particle.

8.4. Particle Above a Metallic Substrate

Other typical and very interesting experimental configurations involving metallic nanoparticles above a metallic substrate were studied in [29, 61]. These had been widely studied before [109, 107, 45] but less attention was paid to the case of the nanoparticle immersed in a medium denser than the vacuum, which is also extensively used in experimental set-ups [63, 79]. The metallic character of both, the particle and the substrate, results in a much more intense interaction between them than was the case for a dielectric substrate, specially for short distances, thereby losing completely the dipolar behavior.

In Figure 8.13, we show the spatial distribution of the electric field around a gold cylinder of radius $R = 25nm$ immersed in water and located above a substrate also made of gold and at distances: $d = 1nm$ (left panel) or $d = 10nm$ (right panel). As in the previous section, three different incident wavelengths have been chosen: well below ($\lambda = 320nm$, first row), well above ($\lambda = 600nm$, bottom row) and in the gold transition regime ($\lambda = 430nm$, middle row) where $|Re(\epsilon_{Au})| \cong 1.69 = (1.3)^2$ (see Figure 8.11). When the distance is short (left panel), as it was outlined in [45], the electric field, due the strong particle-substrate interaction, is concentrated in the gap between them. Then, the distribution differs considerably from the typical "eight-shape" that corresponds to a dipolar behavior. This effect can be observed for wavelengths either below or above the pseudo-matching area, and the electric field acquires values that are $10^3 - 10^4$ times the incident field. On the contrary, when the incident wavelength is such that there is pseudo-matching of both the

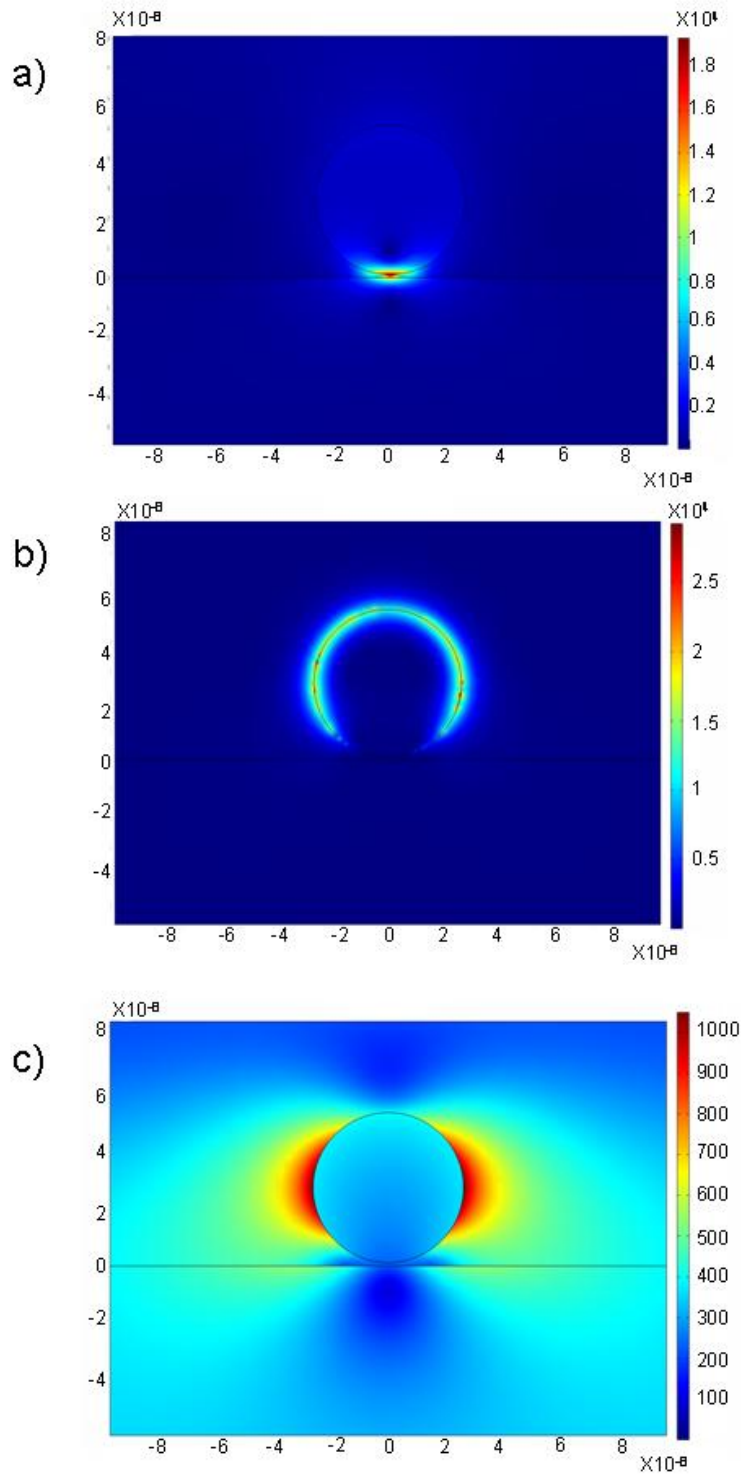


Figure 8.12: Distributions of the electric field around a gold cylinder with radius $R = 25\text{nm}$ embedded in glass ($n = 1.5$) and above a interface with vacuum ($n' = 1$) at a distance $d = 1\text{nm}$ and for three different incident wavelengths: (a) $\lambda = 420\text{nm}$, (b) $\lambda = 496\text{nm}$ (near the matching interval) and (c) $\lambda = 560\text{nm}$

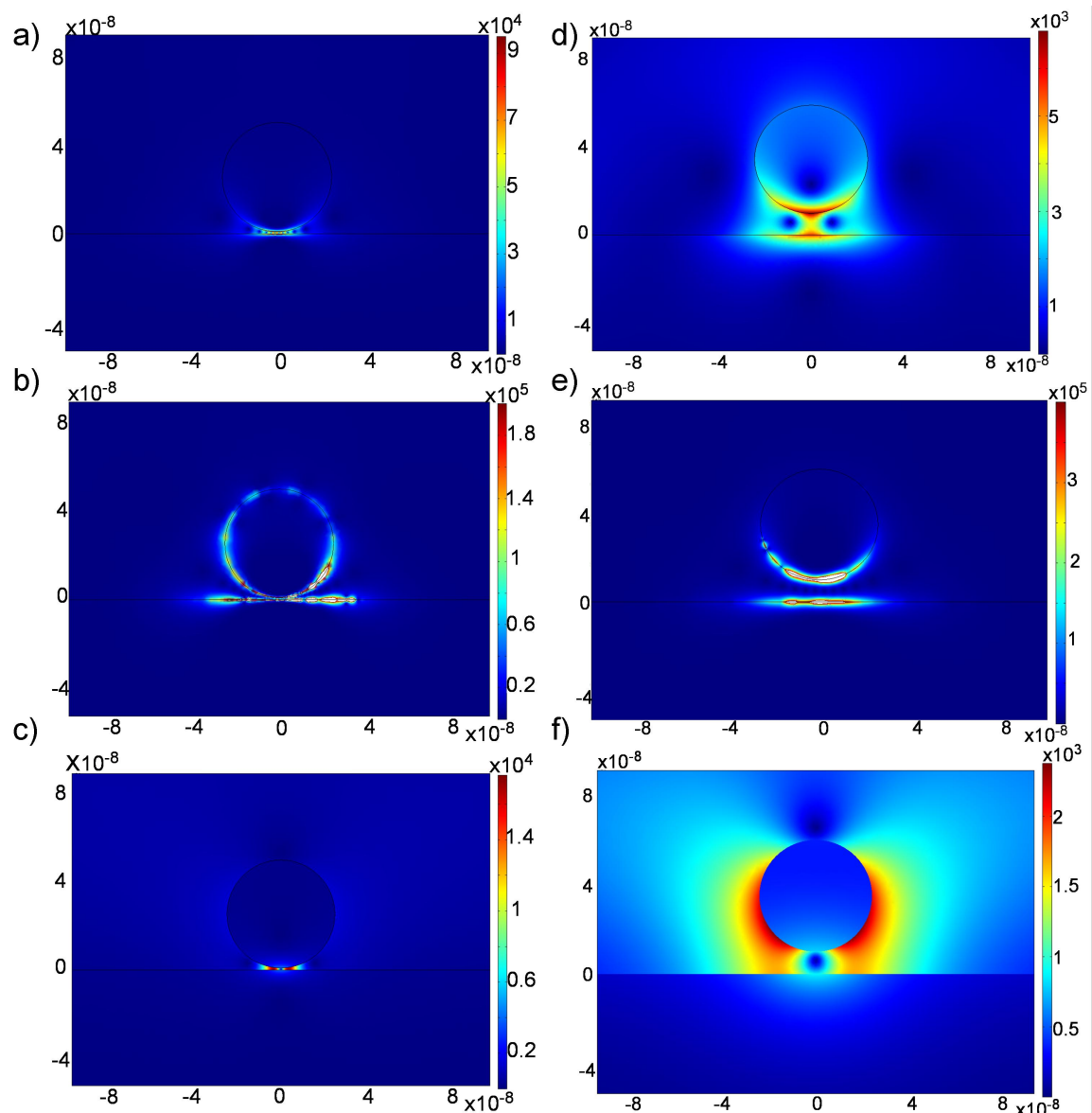


Figure 8.13: Distributions of the electric field around a gold cylinder of radius $R = 25nm$ embedded in water ($n = 1.3$) and above a flat gold surface at a distance $d = 1nm$, (a), (b) and (c) or at $d = 10nm$, (d), (e) and (f) for three different incident wavelengths: (a) and (d) $\lambda = 320nm$, (b) and (e) $\lambda = 430nm$ (near the matching interval) and (c) and (f) $\lambda = 600nm$

cylinder and the substrate with the surrounding medium (Figure 8.13(b)) the distribution of the electric field around the particle is uniform. However, the electric field in the gap is more important than in other points with values as high as $10^5 - 10^6$ times the incident field and even higher concentrations of the electric field can be observed on the surface. As the gap distance increases (right panel), the absolute values of the local electric field decrease and the distribution of it also changes. For λ shorter than the pseudo-matching case (Figure 8.13(d)) the spatial distribution is still concentrated in the part of the cylinder facing the substrate. However, the gap confinement is less important and the surface field spreads out of the bottom part. At $\lambda = 430nm$ (Figure 8.13(e)) the electric field tends to be focused in the gap area, contrary to what happens at closer separations where the surface electric field distribution tends to be uniformly distributed. As in other cases, the pseudo-matching gives values of $|E|$ higher than for other incident wavelengths. Finally, far from the transition area ($\lambda = 600nm$, Figure 8.13(f)), the dipolar behavior and its typical "eight-shape" tend to appear but it is still deformed due to the interaction with the substrate.

8.5. Conclusions

This chapter has been devoted to study the interaction between metallic nanoparticles and a substrate. The analysis has been focused on the evolution of the surface electric field distribution in the presence of this interaction, thereby observing the changes on the typical "eight-shape" (dipolar behavior) as the substrate and the particle are approached. Thereto, we have used a new and fast indicator of these changes: the angular position of the maximum of the local electric field on the surface of the particle (θ_{max}). As it was shown, this parameter is quite sensitive to any perturbation of the dipolar behavior produced by orders higher than the dipolar one or interactions with other structures, such as a substrate in this case.

Firstly and with the purpose of reducing the complexity of the problem, we have stated that, for an isolated nanoparticle, the physics involved in a $2D$ scattering problem is very similar to that of a $3D$ problem. In other words, the results obtained for a $2D$ geometry can be qualitatively extended for a $3D$ geometry. However, to ensure the validity of this extension, several conditions related to the illumination and the polarization of the incident wave must be taken into account.

During the study of this extension, some interesting results have been obtained for the spatial distribution of the local electric field around an isolated and infinite nanocylinder and more specifically for the evolution of the local electric field with different system parameters.

We observed that the maximum of the surface field (θ_{max}) is shifted from the equator of the particle, which corresponds to the typical "eight-shape" of the dipolar behavior, to the forward direction when the particle size increases or when the incident wavelength is able to excite a localized surface plasmon resonance of the system. This feature can also be observed for spherical particles, corroborating the previous generalization of the $2D$ results.

Considering a silver nanocylinder embedded in vacuum, the complex λ -dependence of the refractive index of silver produces an interesting, and also complex evolution of the considered parameter (θ_{max}). For $\lambda < 320nm$, the non-monotonic dependence of the refractive index and the interband transitions of silver in this range, produce flips of θ_{max} which are difficult to explain. This behavior changes when the refractive index of the cylinder and the surrounding medium match. At this point the angular position of the maximum of the electric field runs to 0° remaining there for a certain spectral range. Both the flip wavelength and the spectral range depend on the particle size and the refractive index of the surrounding medium. For larger incident wavelengths, the well-defined metallic character of silver and the small ratio (R/λ) of the dipolar behavior, the dominant one and θ_{max} tends to 90° . This behavior is similar to that of a gold cylinder or a gold sphere. In the considered spectral range, gold presents a well-defined metallic character without matching the surrounding medium. Because of that, θ_{max} is fixed in the neighborhood of 90° along the whole range of wavelengths.

The near-field distribution changes considerably if a dielectric substrate (glass in our case) is approached to the nanostructure. This fact produces a concentration of the electric field in the gap which remains stable as the distance decreases, that is, when the maximum θ_{max} tends to be located at 0° (the part facing the substrate) for a longer range of wavelengths. More interesting is the evolution of the electric field distributions as the gap distance changes for a certain wavelength: when the nanoparticles is far from the substrate and they do not interact, the typical "eight-shape" of the dipolar behavior is manifested with two maxima at $\theta_{max} = 90^\circ$ and $\theta_{max} = 270^\circ$. As d decreases, the interaction shifts these maxima towards the forward direction ($\theta_{max} = 0^\circ$). This implies a strong concentration of the electric field in the gap, which could be useful for nanolithography applications. As we have mentioned, the value of λ at which the particle starts to behave as a dipole, is dependent on surrounding medium. Embedding the nanoparticle in a medium denser than the substrate, makes the electric field tending to a dipolar behavior for shorter wavelengths than in air.

Finally, we have reproduced a configuration commonly found in experimental set-ups, consisting of a metallic particle (a gold cylinder in our case) embedded in a medium denser than vacuum (typically water) and located above a metallic substrate (made of gold in our

calculations). The metallic character of both the particle and the surface, makes the interaction much stronger than for the case of a dielectric substrate. Hence, the concentration of the surface electric field in the gap can be observed for wavelengths well below and well above of the transition region (at which the refractive index of the cylinder and the surrounding medium match). In this case the matching of the refractive index is between the cylinder, the surrounding medium and also the substrate (made of the same material as the cylinder). Because of that, the spatial distribution of the local electric field is uniform around the particle close to this pseudo-matching, acquiring high values. As the gap distance increases, the values of the electric field decreases, the level of localization of the surface field in the gap is less important and above the pseudo-matching wavelength, the particle tends to the dipolar behavior.

Conclusions and Further Ideas

"Ladran, luego cabalgamos"
—Sentencia griega erróneamente atribuida a
Miguel de Cervantes

To finish this thesis, we would like to summarize our results and the main conclusions of this work. We also point out several ideas which have arisen during these years, and which can constitute the basis for further researches.

9.1. Summary and Conclusions

During the last years, a new and fascinating research field has arisen around light scattering by nanostructures and its applications. This is *Plasmonics*. It considers metallic media for which resonant behaviors in the visible part of the spectrum are observed. Several studies and applications based on this have risen [10, 17, 19, 68, 5, 67]. In addition, new artificial engineered materials, known as *metamaterials*, have been developed such that electric and magnetic effective properties can be observed in the same range of wavelengths. These new media allow to observe scattering features, never detected before, and which would be the base of several new applications [32, 42, 26, 33, 34, 66]. These new advances motivated us to focus our attention on those aspects.

In order to simplify the problem, we considered spherical particles with a size (R) much smaller than the incident wavelength (λ) and with arbitrary values for the optical constants, including the interesting double-negative range ($\epsilon < 0$ and $\mu < 0$). Although this kind of particle is completely unrealistic nowadays, researchers are obtaining metamaterials, made of small subunits such that macroscopically, the material can be considered as continuous with effective optical properties. We fully agree that complex computational methods, which consider the inner structure of media, are more accurate than ours, however, in our mind, a simple system is adequate to understand the physics involved in the problem.

In the first part of the thesis, a single, isolated, spherical and small particle is considered. By changing its size and optical properties (ϵ, μ) we have observed quite interesting scattering features.

- Resonant light scattering by spherical particles and their evolution as a function of their optical constants and their size were studied in detail with our own approximate expressions for the first four Mie coefficients, including dipolar and quadrupolar electric and magnetic modes of charge distribution. As was shown, we observed that light scattering resonances are connected along the range of values for (ϵ, μ) and that even electric-magnetic symmetries can be observed. When $(\epsilon, \mu) = (-2, -2)$, an electric and a magnetic dipolar resonance overlap generating an important enhancement in the light scattering unconventional characteristics. These values for the optical constants will be a referent along this work.
- Several years ago, light scattering by small particles with arbitrary values for the permittivity and permeability was analyzed by Kerker et al [69]. They stated that a control of the directionality of light scattering could be possible by tuning the optical constants. Much of our efforts are based on their discoveries and we have tried to generalize their work. We show that similar directional conditions can be obtained for finite-sized particles, still smaller than λ , and for scattering angles different from those studied before ($\theta = 0^\circ$ and $\theta = 180^\circ$). In addition, it is well-known that the spatial distribution of light scattering is dependent on the observation distance. For this reason, the considered directional conditions have been analyzed as a function of the distance between the diffuser and the observer, from the near- to the far-field regions. From our calculations we can conclude that while the angular distribution of the scattered intensity can be controlled in the far field by tuning the optical constants, in the near-field region, the dipolar character of these small particles dominates.

The second part is devoted to aggregates of particles studied in the previous part of this work. Using the so-called Coupled Electric and Magnetic Dipole Method (CEMDM), we have observed the influence of multiple scattering processes in the directional conditions for the scattered light. In addition, a design of a new left-handed system composed of both electric and magnetic particles and which does not scatter in the backward direction is considered and analyzed in detail as a function of different geometrical parameters.

In the last part of the thesis we considered a different way to manipulate the scattering pattern of a single particle. In this case, we have shown that useful alterations of the spatial distribution of the dipolar resonance of a metallic cylinder can be obtained by changing the distance between the cylinder and a substrate underneath.

9.2. Further Ideas

Although this thesis was designed to be a complete study about light scattering by nanoparticles with arbitrary values for the optical constants, and more specifically focused on the manipulation of the directionality of light scattered by them, many issues could not be addressed, either by space or time requirements. We shall therefore describe some of those ideas here:

- First, this work can be carried out using more complex computational techniques in order to obtain quantitative results and not only qualitative ones. Hence, a more complex method will allow to increase the particle size to observe multipolar behaviors.
- In the last years, materials with epsilon-near-zero (ENZ) or epsilon-very-large (EVL) have been developed. Particles with ϵ and μ in these ranges could be very interesting to analyze.
- Our calculations on systems of nanoparticles were reduced to dimers due to computational requirements. Larger systems with aligned or non-aligned arrangements should be taken into account. The design of nanocircuits could be used as a reference for this kind of studies.
- Finally, other aspects such as polarimetry are also interesting. For instance, estimations of the degree of linear polarization in particles with electric and magnetic properties are currently underway.

Resumen en castellano

El estudio de la luz difundida por un cierto sistema ha resultado ser una técnica no invasiva de gran interés en diversos campos, desde la biología a la meteorología pasando por las energías renovables. En los últimos años han surgido una gran cantidad de aplicaciones basadas en la misma. Y es que, del análisis de las propiedades de la luz difundida (intensidad, polarización, distribución espacial) se puede obtener valiosa información sobre las propiedades del medio difusor, tanto ópticas como geométricas. Esto es lo que se ha venido en llamar el *Problema Inverso*.

Los fenómenos derivados de la interacción entre la luz y la materia han sido largamente estudiados. En particular, los últimos trabajos sobre la interacción de la luz con estructuras metálicas, que pueden originar la excitación de resonancias plasmónicas, y de la luz con los nuevos materiales nanoestructurados, o metamateriales, han servido de inspiración para el presente estudio.

Objetivo

En el trabajo presentado se han analizado, desde un punto de vista numérico, los efectos y/o fenómenos observables en la luz difundida por pequeñas partículas con constantes ópticas tanto convencionales (principalmente metálicas) como no convencionales (partículas con

respuesta magnética en el rango del visible). En particular, nos hemos centrado en los efectos en la direccionalidad de la luz difundida observados en el análisis aplicado tanto a partículas aisladas como a agregados de las mismas. Este estudio puede considerarse como un paso previo hacia el desarrollo de nuevas aplicaciones en circuitos ópticos o tratamientos médicos basados en nanopartículas.

Con el fin de extraer con cierta facilidad la física del problema, sin necesidad de complejos modelos matemáticos, hemos usado un modelo simple basado en pequeñas partículas (cuyo radio es mucho menor que la longitud de onda incidente) con simetría esférica y propiedades ópticas (ϵ, μ) arbitrarias. El rango $(\epsilon < 0, \mu < 0)$, en el cuál se encuadran los materiales "zurdos", ha sido estudiado con especial atención.

En una primera parte, nuestro análisis se ha limitado al caso de una partícula aislada, para cuyo estudio hemos usado la teoría de Mie. Debido al tamaño de las partículas ($R \ll \lambda$) sólo la contribución debida a los primeros cuatro términos de la expansión de Mie (a_1, b_1, a_2 y b_2) se ha considerado, siendo despreciable aquella debida a términos de orden mayor. Tras un pormenorizado análisis de cómo difunde una pequeña partícula con propiedades ópticas arbitrarias, nuestro estudio se ha centrado en la posibilidad de controlar la direccionalidad de la luz difundida por las mismas. Para este fin hemos seguido los estudios realizados por Kerker et al [69] para partículas dipolares ($R \rightarrow 0$), extendiéndolos a partículas de tamaño finito y a cualesquiera dirección de difusión, tanto en el rango de campo cercano como en el de campo lejano.

Si bien, las partículas tienden a formar agregados, por lo que, en una segunda parte, hemos abordado el análisis de la direccionalidad de la luz difundida por un agregado de las partículas descritas en la primera parte. De nuevo y con el fin de simplificar la matemática del problema, hemos considerado o bien el agregado más simple, el dímero, o bien arrays de partículas tales que la aproximación dipolar sea aplicable en ellos. Esta aproximación permite calcular los campos difundidos por las partículas, teniendo en cuenta las interacciones entre ellas, mediante el Método del Dipolo Eléctrico y Magnético Acoplado (*CEMDM* en sus siglas en inglés).

Finalmente el trabajo da un giro para tratar un tema más realista, experimentalmente hablando, aunque tangencialmente relacionado con todo lo anterior. Y es que, como se muestra, la distribución espacial del campo difundido por una nanopartícula metálica en resonancia (resonancia plasmónica localizada) puede ser modificada por la presencia de un substrato (tanto dieléctrico como metálico) bajo la misma.

Esquema del trabajo

Los dos primeros capítulos de este trabajo se han dedicado a introducir brevemente el problema a tratar. Así, mientras el primer capítulo hace un repaso sobre la historia y los conceptos básicos en la interacción entre la luz y la materia, exponiendo, a su vez, los objetivos que nos hemos marcado, en el capítulo 2 se desgana la teoría relativa a la difusión de la luz por una partícula aislada.

Tras estos dos capítulos introductorios, y tal como se ha comentado anteriormente, el trabajo se divide en tres partes. En la primera parte tratamos el problema de la difusión de la luz por pequeñas partículas aisladas con propiedades ópticas arbitrarias. En la segunda parte, extendemos el problema a sistemas de partículas. Y en la tercera y última parte, la geometría a estudiar consiste en una partícula metálica en presencia de un sustrato.

En el capítulo 3, llevamos a cabo el análisis de las resonancias de Mie en pequeñas partículas con propiedades ópticas en los cuatro posibles cuadrantes: $(\epsilon > 0, \mu > 0)$, $(\epsilon < 0, \mu > 0)$, $(\epsilon < 0, \mu < 0)$ y $(\epsilon > 0, \mu < 0)$. El rango doble-negativo, $(\epsilon < 0, \mu < 0)$, es el que mayor interés ha suscitado dada la cantidad de fenómenos y/o aspectos observados en la misma: resonancias tanto de dipolares como cuadrupolares, eléctricas y/o magnéticas, una simetría $\epsilon - \mu$, así como un punto de gran interés $(\epsilon = \mu = -2)$ que va a ser un referente a lo largo de todo el trabajo.

El capítulo 4 engloba los resultados sobre la direccionalidad de la luz difundida por una partícula aislada. En éste se estudia la influencia que un tamaño de partícula finito tiene sobre las condiciones de direccionalidad de Kerker [69]. Estas condiciones establecen que cuando las constantes ópticas de un pequeño difusor esférico verifican una de ellas, la difusión hacia adelante o en retrodifusión es anulada. No obstante, como nosotros mostramos, la luz difundida también puede ser eliminada en otras direcciones, bajo condiciones similares para las constantes ópticas. Por último, en este apartado se demuestra como el punto de interés antes comentado, $(\epsilon = \mu = -2)$, supone una excepción a la condición de Kerker sobre la difusión hacia adelante.

El capítulo 5 y último de la primera parte, aborda la dependencia que las condiciones de Kerker tienen con la distancia de observación. Para mostrar esta dependencia hemos calculado los diagramas de difusión de una partícula bajo dichas condiciones para distintas distancias de observación, tanto en el rango de campo cercano (pequeñas distancias) como en el campo lejano (largas distancias).

El capítulo 6 y primero de la segunda parte del trabajo, muestra los principales resulta-

dos que hemos obtenido para un dímero de partículas con constantes ópticas que verifiquen alguna de las condiciones de direccionalidad. Con este estudio hemos pretendido ir un paso más allá en el análisis del control sobre la luz difundida, así como observar la influencia que las interacciones entre partículas cercanas tiene sobre dicha direccionalidad. Como en el caso anterior, para este estudio hemos considerados distancias de observación tanto en el rango de campo cercano como en el campo lejano. Mientras que para largas distancias (campo lejano) la aproximación dipolar es adecuada y suficiente para obtener, con suficiente precisión, los campos difundidos por el dímero, para cortas distancias (campo cercano) hemos usado un método más complejo basado en ecuaciones integrales de superficie (en inglés: surface integral equations o SIE).

En el capítulo 7 presentamos el diseño de un sistema compuesto por partículas, tanto eléctricas como magnéticas, que interaccionan entre sí. Para una cierta configuración geométrica, hemos demostrado que el sistema completo difunde luz de igual modo que una única partícula aislada cuya permitividad eléctrica (ϵ) es igual a la de las partículas eléctricas del sistema y cuya permeabilidad magnética (μ) es igual a la de las partículas magnéticas del agregado. Las propiedades ópticas de las partículas fueron escogidas tales que se obtuviera mínima retrodifusión, cuya persistencia es analizada en función de ciertos parámetros geométricos (tamaño y posición de las partículas, distancias, etc.).

La última parte de la tesis consta de un único capítulo, el capítulo 8. En éste mostramos cómo la presencia de un sustrato plano, tanto metálico como dieléctrico, es capaz de alterar la distribución dipolar de un cilindro metálico (hecho de oro o plata) en resonancia. La presencia del sustrato induce una importante localización del campo eléctrico entre ambas estructuras. Localización que depende tanto de la distancia entre las mismas como de la naturaleza del sustrato, del medio circundante y de la longitud de onda incidente. El cilindro considerado es infinitamente largo y de sección circular con un radio mucho menor que la longitud de onda incidente. No obstante, tal y como mostramos en este capítulo, estos resultados pueden extenderse, con ciertas precauciones, al caso de una nanopartícula esférica.

Finalmente y para concluir, el último capítulo resume los principales resultados y conclusiones obtenidos, además de explicar cuáles son las perspectivas futuras de este trabajo.

Publications and Conferences

Chapters on Books

- B. García-Cámara, "Intra-/Inter-Chip Optical Communications: High Speed and Low Dimensions", *Communications Architectures for Systems-on-Chip* , J.L. Ayala ed. Taylor and Francis, in press.

Peer-Reviewed Articles

- B. García-Cámara, F. Moreno, F. González and J. M. Sáiz, *Comment on "Experimental evidence of zero forward scattering by magnetic spheres"*, Phys. Rev. Lett. **98**, 179701 (2007).
- B. García-Cámara, F. Moreno, F. González, J. M. Sáiz and G. Videen, *Light Scattering Resonances in Small Particles with Electric and Magnetic Properties*, J. Soc. Am. A **25**, 327-334 (2008).
- B. García-Cámara, F. González, F. Moreno, and J. M. Sáiz, *Exception for the zero-forward scattering theory*, J. Soc. Am. A **25**, 2875-2878 (2008).

- F. Moreno, B. García-Cámara, J. M. Sáiz and F. González, *Interaction of nanoparticles with substrates: effects on the dipolar behaviour of the particles*, Opt. Express **16**, 12487-12504 (2008).
- B. García-Cámara, J.M. Sáiz, F. González and F. Moreno, *Nanoparticles with unconventional scattering properties*, Opt. Commun. **283**, 490-496 (2010)
- B. García-Cámara, J.M. Sáiz, F. González and F. Moreno, *Distance limit of the directionality conditions for the scattering of nanoparticles*, Metamaterials **4**, 15-23 (2010).
- B. García-Cámara, F. Moreno, F. González and O. J. F. Martin, *Light scattering by an array of electric and magnetic nanoparticles* Opt. Express **18**, 10001-10015 (2010)
- B. García-Cámara, F. González and F. Moreno, *On the Fröhlich frequency for nanoparticles with non-conventional optical properties*, (in preparation).

Contributions to Conferences

- **Authors:** B. García-Cámara, F. González, F. Moreno and J.M. Sáiz
Title: *Resonances in Light Scattering by Small Particles*
Kind of participation: poster
Conference: Photonic Metamaterials: From Random to Periodic
Date: June 2006
Place: Grand Bahama Island (Bahamas)
- **Authors:** B. García-Cámara, F. González, F. Moreno, J.M. Sáiz and G. Videen
Title: *Resonancias de Mie en Partículas con Permeabilidad Magnética Negativa*
Kind of participation: poster
Conference: 8ª Reunión Nacional de Óptica
Date: September 2006
Place: Alicante (Spain)
- **Authors:** F. Moreno, B. García-Cámara, F. González and J.M. Sáiz
Title: *Interaction of Nanoparticles with Substrates: Effects on Dipolar Behaviour of the Particles*

Kind of participation: poster

Conference: III International Conference on Surface Plasmon Photonics

Date: June 2007

Place: Dijon (France)

- **Authors:** B. García-Cámara, F. González, F. Moreno and J.M. Sáiz

Title: *Zero-forward scattering by Nanoparticles*

Kind of participation: poster

Conference: I Conferencia Española de Nanofotónica

Date: April 2008

Place: Tarragona (Spain)

- **Authors:** B. Setién, B. García-Cámara, F. Moreno, F. González and J.M. Sáiz

Title: *Light-Scattering Depolarization by Metallic Nanoparticles: Size Dependence*

Kind of participation: poster

Conference: 9th International Conference in Nanostructured Materials

Date: June 2008

Place: Rio de Janeiro (Brasil)

- **Authors:** B. García-Cámara, F. Moreno, F. González, J.M. Sáiz and G. Videen

Title: *Mie resonances in small particles with electric and magnetic properties*

Kind of participation: poster

Conference: Progress in Electromagnetic Research Symposium (PIERS)

Date: July 2008

Place: Cambridge (USA)

- **Authors:** B. García-Cámara, F. González, F. Moreno and J.M. Sáiz

Title: *Extended zero forward scattering condition by nanoparticles*

Kind of participation: poster

Conference: 11th Electromagnetic and Light Scattering Conference

Date: September 2008

Place: London (UK)

- **Authors:** B. Setién, B. García-Cámara, F. González, F. Moreno and J.M. Sáiz
Title: *Analysis of high order resonances in metallic nanoparticles by polarimetric techniques*
Kind of participation: poster
Conference: 11th Electromagnetic and Light Scattering Conference
Date: September 2008
Place: London (UK)

- **Authors:** B. García-Cámara, J.M. Sáiz, F. González and F. Moreno
Title: *Directional scattering behavior of systems of nanoparticles with double negative optical properties*
Kind of participation: poster
Conference: NanoSpain 2009
Date: March 2009
Place: Zaragoza (Spain)

- **Authors:** B. García-Cámara, J.M. Sáiz, F. González and F. Moreno
Title: *Directional scattering behavior of systems of nanoparticles with non-conventional optical properties*
Kind of participation: poster
Conference: IV International Conference on Surface Plasmon Polaritons
Date: June 2009
Place: Amsterdam (Netherlands)

- **Authors:** B. Setién, B. García-Cámara, J.M. Sáiz, F. González and F. Moreno
Title: *Influence of higher order modes on the polarimetric properties of a metallic nanodimer*
Kind of participation: poster
Conference: IV International Conference on Surface Plasmon Polaritons
Date: June 2009
Place: Amsterdam (Netherlands)

- **Authors:** B. García-Cámara, J.M. Sáiz, F. González and F. Moreno

Title: *Sistemas de Nanopartículas con Índice de Refracción Negativo*

Kind of participation: poster

Conference: 9^a Reunión Nacional de Óptica

Date: September 2009

Place: Ourense (Spain)

- **Authors:** B. García-Cámara, A. Kern, F. Moreno, F. González and O.J.F. Martin
Title: *Near-Field Scattering by Nanoparticles with Unconventional Scattering Properties*
Kind of participation: oral
Conference: 2nd International Conference on Metamaterials, Photonic Crystals and Plasmons
Date: February 2010
Place: Cairo (Egypt)
- **Authors:** B. García-Cámara, F. Moreno, F. González and O.J.F. Martin
Title: *Light Scattering by an Array of Nanoparticles with Electric and Magnetic Properties*
Kind of participation: poster
Conference: 2nd International Conference on Metamaterials, Photonic Crystals and Plasmons
Date: February 2010
Place: Cairo (Egypt)
- **Authors:** B. García-Cámara, F. González and F. Moreno
Title: *Size Evolution of the Fröhlich Resonance for Magnetic Nanoparticles*
Kind of participation: oral
Conference: 2^a Conferencia Española de Nanofotónica
Date: June 2010
Place: Segovia (Spain)
- **Authors:** F. Moreno, P. Albella, F. González and B. García-Cámara
Title: *Fundamentos de Espectroscopía Plasmónica con Nanopartículas Metálicas*

Kind of participation: oral

Conference: Plasmónica: Detección sobre Nanoestructuras Metálicas

Date: June 2010

Place: Jaca (Spain)

- **Authors:** B. García-Cámara, F. González and F. Moreno

Title: *Scattering of Light by a Dimer of Nanoparticles with Unconventional Optical Properties: from Far to Near Field*

Kind of participation: poster

Conference: NATO Advanced Study Institute on "Special Detection Technique (Polarimetry) and Remote Sensing"

Date: September 2010

Place: Hyiv (Ukraine)

Bibliography

- [1] <http://www.biacore.com/lifesciences/index.html>.
- [2] <http://www.reichertspr.com/index.html>.
- [3] S. Abalde-Cela, P. Aldeanueva-Potel, C. Mateo-Mateo, L. Rodríguez-Lorenzo, R.A. Alvarez-Puebla, and L.M. Liz-Marzán. Surface-enhanced Raman scattering biomedical applications of plasmonic colloidal particles. *J. R. Soc. Interface*, doi: 10.1098/rsif.2010.0125.focus, 2010.
- [4] M. Abramowitz and I. A. Stegun. *Handbook of Mathematical Functions*. Dover Publications Inc., New York, 9th edition, 1970.
- [5] S. Aćimović, M.P. Kreuzer, M.U. González, and R. Quidant. Plasmon near-field coupling in metal dimers as a step toward single-molecule sensing. *ACS Nano*, 3(5):1231–1237, 2009.
- [6] Y.A. Akimov, W.S. Koh, S.Y. Sian, and S. Ren. Nanoparticle-enhanced thin film solar cells: Metallic or dielectric nanoparticles? *Appl. Phys. Lett.*, 96(7):073111, 2010.
- [7] V.R. Almeida, C.A. Barrios, and R.R. Panepucci. All-optical control of light on a silicon chip. *Nature*, 431:1081–1084, 2004.

- [8] A. Alù and N. Engheta. The quest for magnetic plasmons at optical frequencies. *Opt. Express*, 17(7):5723–5730, 2009.
- [9] A. Alù and N. Engheta. How does zero forward-scattering in magnetodielectric nanoparticles comply with the optical theorem? *J. Nanophoton.*, 4(1):041590, 2010.
- [10] J.N. Anker, W.P. Hall, O. Lyandres, N.C. Shah, J. Zhao, and R.P. Van Duyne. Biosensing with plasmonic nanosensors. *Nature Mat.*, 7:442–453, 2008.
- [11] F. González B. García-Cámara, F. Moreno, and J. M. Saiz. Exception for the zero-forward-scattering theory. *J. Opt. Soc. Am. A*, 25(11):2875–2878, 2008.
- [12] V. Backman et al. Detection of preinvasive cancer cells. *Nature*, 406:35–36, 2000.
- [13] P. W. Barber and S. C. Hill. *Light Scattering by Particles: Computational Methods*. World Scientific, Singapore, 1990.
- [14] C. F. Bohren and D. R. Huffman. *Absorption and Scattering of Light by Small Particles*. John Wiley and Sons, New York, 1983.
- [15] A. Boltasseva and V.M. Shalaev. Fabrication of optical negative-index metamaterials: Recent advances and outlook. *Metamaterials*, 2(1):1–17, 2008.
- [16] J.A. Bossard, S. Yun, D.H. Werner, and T.S. Mayer. Synthesizing low loss negative index metamaterial stacks for mid-infrared using genetic algorithms. *Opt. Express*, 17(17):14771–14779, 2009.
- [17] Y.C. Cao, R. Jin, and C.A. Mirkin. Nanoparticles with Raman spectroscopic fingerprints for DNA and RNA detection. *Science*, 297:1536–1540, 2002.
- [18] J. Casas. *Óptica*. Librería PONS, Zaragoza, 7th edition, 1994.
- [19] K.R. Catchpole and A. Polman. Plasmonic solar cells. *Opt. Express*, 16:21793–21800, 2008.
- [20] P.C. Chaumet and A. Rahmani. Coupled-dipole method for magnetic and negative-refraction materials. *J. Quant. Spec. Rad. Trans.*, 110:22–29, 2009.
- [21] P.C. Chaumet, A. Rahmani, F. de Fornel, and J.-P. Dufour. Evanescent light scattering: the validity of the dipole approximation. *Phys. Rev. B*, 58(4):2310–2315, 1998.

- [22] H. Chen, C.T. Chan, and P. Sheng. Transformation optics and metamaterials. *Nature Mat.*, 9:387–396, 2010.
- [23] P. Chýlek. Asymptotic limits of the Mie-scattering characteristics. *J. Soc. Am.*, 65(11):1316–1318, 1975.
- [24] P. Chýlek and R.G. Pinnick. Nounitariness of the light scattering approximations. *Appl. Phys.*, 18(8):1123–1124, 1979.
- [25] J.L. de la Peña, F. González, J.M. Saiz, F. Moreno, and P.J. Valle. Sizing particles on substrates. A general method of oblique incidence. *J. Appl. Phys.*, 85(1):432–438, 1999.
- [26] M.R. Dennis. Metamaterials: A cat’s eye for all directions. *Nature Mat.*, 8:613–614, 2009.
- [27] A. Dhawan, S. Norton, M. Gerhold, and T. Vo-Dinh. Comparison of FDTD numerical computations and analytical multipole expansion method for plasmonic-active nanosphere dimers. *Opt. Express*, 17:9688–9703, 2009.
- [28] B.T. Draine and P.J. Flatau. Discrete-dipole approximation for scattering calculations. *J. Opt. Soc. Am. A*, 11(4):1491–1499, 1994.
- [29] J. D. Driskell, R. J. Lipert, and M.D. Porter. Labeled gold nanoparticles immobilized at a smooth metallic substrate: Systematic investigation of surface plasmon resonances and surface-enhanced Raman scattering. *J. Phys. Chem. B*, 110(35):17444–17451, 2006.
- [30] A. Einstein. Über einen die Erzeugung und Verwandlung des Lichtes betreffenden heuristischen Gesichtspunkt. *Annalen der Physik*, 17:132–148, 1905.
- [31] Y. Ekinici, A. Christ, M. Agio, O.J.F. Martin, H.H. Solak, and J.F. Löffler. Electric and magnetic resonances in arrays of coupled gold nanoparticles in-tandem pairs. *Opt. Express*, 16(17):13287–13295, 2008.
- [32] N. Engheta. Circuits with Light at Nanoscales: Optical Nanocircuits Inspired by Metamaterials. *Science*, 317(5845):1698–1702, 2007.
- [33] T. Ergin, N. Stenger, P. Brenner, J.B. Pendry, and M. Wegener. Three-dimensional invisibility cloak at optical wavelengths. *Science*, 328:337–339, 2010.

- [34] A. Fang, T. Koschny, and C. M. Soukoulis. Lasing in metamaterial nanostructures. *J. Opt.*, 12(2):024013, 2010.
- [35] V.E. Ferry, L.E. Sweatlock, D. Pacifici, and A. Atwater. Plasmonic nanostructure design for efficient light coupling into solar cells. *Nano Lett.*, 8(12):4391–4397, 2008.
- [36] A.S. Funston, C. Novo, T.J. Davis, and P. Mulvaney. Plasmon coupling of gold nanorods at short distances and different geometries. *Nano Lett.*, 9(4):1651–1658, 2009.
- [37] J.K. Gansel, M.Thiel, M.S. Rill, M. Decker, K. Bade, V. Saile, G. von Freymann, S. Linden, and M. Wegener. Gold helix photonic metamaterial as broadband circular polarizer. *Science*, 325:1513–1515, 2009.
- [38] N. García and M. Nieto-Vesperinas. Left-handed materials do not make a perfect lens. *Phys. Rev. Lett.*, 88(20):207403, 2000.
- [39] B. García-Cámara, F. Moreno, F. González, J. M. Saiz, and G. Videen. Light scattering resonances in small particles with electric and magnetic properties. *J. Opt. Soc. Am A*, 25:327–334, 2008.
- [40] B. García-Cámara, J.M. Saiz, F. González, and F. Moreno. Nanoparticles with unconventional scattering properties: Size effects. *Opt. Commun.*, 283:490–496, 2010.
- [41] F.J. García-Vidal, L. Martín-Moreno, T.W. Ebbesen, and L. Kuipers. Light passing through subwavelength apertures. *Reviews of Modern Physics*, 82(1):729–787, 2010.
- [42] T.K. Gaylord, J.L. Stay, and J.D. Meindl. Optical interconnect devices and structures based on metamaterials. *US patent*, 2008/0212921, 2008.
- [43] P. Genuche, S. Cherukulappurath, T.H. Taminiau, N.F. van Hulst, and R. Quidant. Spectroscopic mode mapping of resonant plasmon nanoantennas. *Phys. Rev. Lett.*, 101:116805, 2008.
- [44] V. Giannini and J.A. Sánchez-Gil. Excitation and emission enhancement of single molecule fluorescence through multiple surface-plasmon resonances in metal trimer nanoantennas. *Opt. Lett.*, 33:899–901, 2008.
- [45] G.Lévêque and O.J.F. Martin. Optical interactions in a plasmonic particle couple to a metallic film. *Opt. Express*, 14:9971–9981, 2006.

- [46] D.Ö. Güney, T. Koschny, M. Kafesaki, and C. M. Soukoulis. Connected bulk negative index photonic metamaterials. *Opt. Lett.*, 34(4):506–508, 2009.
- [47] E. Hao and G.C. Schatz. Electromagnetic fields around silver nanoparticles and dimers. *J. Chem. Phys.*, 120(1):357–366, 2003.
- [48] E. Hao and G.C. Schatz. Electromagnetic fields around silver nanoparticles and dimers. *J. Chem. Phys.*, 120(1):357–366, 2004.
- [49] R.F. Harrington. *Field Computation by Moment Methods*. Macmillan, 1968.
- [50] M. Haurylau, G. Chen, H. Chen, J. Zhang, N.A. Nelson, D.H. Albonese, E.G. Friedman, and P.M. Fauchet. On-chip optical interconnect roadmap: challenges and critical directions. *IEEE J. Sel. Top. Quant. Elec.*, 12:1699–1709, 2006.
- [51] O. Hess. Optics: Farewell to Flatland. *Nature*, 455:299–300, 2008.
- [52] L.B. Hirsch, J.B. Jackson, A. Lee, and N.J. Halas. A whole blood immunoassay using gold nanoshells. *Anal. Chem.*, 75:2377–2381, 2003.
- [53] C. L. Holloway, E.F. Kuester, J. Baker-Jarvis, and P. Kabos. A double negative (DNG) composite medium composed of magnetodielectric spherical particles embedded in a matrix. *IEEE Trans. Antennas Propagat.*, 51:2596–2603, 2003.
- [54] C.L. Holloway, M.A. Mohamed, E.F. Kuester, and A. Dienstfrey. Reflection and transmission properties of a metal film: with an application to a controllable surface composed of resonant particles. *IEEE Trans. Electromag. Compat.*, 47:853–865, 2005.
- [55] J. Homola. *Surface Plasmon Resonance Based Sensors*. Springer-Verlag, New York, 2006.
- [56] X. Huang, P.K. Jain, I.H. El-Sayed, and M.A. El-Sayed. Plasmonic photothermal therapy (PPTT) using gold nanoparticles. *Lasers in Med. Sci.*, 23(3):217–228, 2008.
- [57] J. D. Jackson. *Classical Electrodynamics*. Wiley, New York, 1975.
- [58] J.B. Jackson and N.J. Halas. Silver nanoshells variation in morphologies and optical properties. *J. Phys. Chem.*, 105:2743–2746, 2001.
- [59] J.B. Jackson and N.J. Halas. Surface-enhanced Raman scattering on tunable plasmonic nanoparticle substrates. *PNAS*, 101(52):17930–17935, 2004.

- [60] P.B. Johnson and R.W. Christy. Optical constants of the noble metals. *Phys. Rev. B*, 6:4370–4379, 1972.
- [61] S. Joo and D.F. Baldwin. Adhesion mechanisms of nanoparticle silver to substrate materials: identification. *Nanotech.*, 21:055204, 2010.
- [62] A.V. Kabashin, P. Evans, S. Pastkovsky, W. Hendren, G.A. Wurtz, R. Atkinson, R. Pollard, V.A. Podolskiy, and A.V. Zayats. Plasmonic nanorod metamaterials for biosensing. *Nature Mat.*, 8:867–871, 2009.
- [63] T. Kalkbrenner, U. Håkanson, and V. Sandoghdar. Tomographic plasmons spectroscopy of a single gold nanoparticle. *Nano Lett.*, 4:2309–2314, 2004.
- [64] T. Kalr, M. Perner, S. Grosse, G. von Plessen, W. Spirkl, and J. Feldmann. Surface-plasmon resonances in single metallic nanoparticles. *Phys. Rev. Lett.*, 80:4249–4252, 1998.
- [65] B. Kanté, A. de Lustrac, J.-M. Lourtioz, and F. Gadot. Engineering resonances in infrared metamaterials. *Opt. Express*, 16(10):6774–6784, 2008.
- [66] T.S. Kao, F.M. Huang, Y. Chen, E.T.F. Rogers, and N.I. Zheludev. Metamaterial as a controllable template for nanoscale field localization. *Appl. Phys. Lett.*, 96:041103, 2010.
- [67] S. Kawata, Y. Inouye, and P. Verma. Plasmonics for near-field nano-imaging and superlensing. *Nature Phot.*, 3(7):388–394, 2009.
- [68] S. Kawata, A. Ono, and P. Verma. Subwavelength colour imaging with a metallic nanolens. *Nature Phot.*, 2:438–442, 2008.
- [69] M. Kerker, D.-S. Wang, and C.L. Giles. Electromagnetic scattering by magnetic spheres. *J. Opt. Soc. Am.*, 73:765–767, 1983.
- [70] A. Kern and O.J.F. Martin. Surface integral formulation for 3-D simulations of plasmonic and high permittivity nanostructures. *J. Opt. Soc. Am*, 26(4):732–740, 2009.
- [71] A.M. Kern and O.J.F. Martin. Modelling near-field properties of plasmonic nanoparticles: a surface integral approach. *Proc of SPIE*, 7395:739518, 2009.
- [72] P.G. Kik, S.A. Maier, and H.A. Atwater. Plasmon printing: A new approach to near-field lithography. *Mater. Res. Soc. Symp. Proc.*, 705:66–71, 2002.

- [73] A. Kinkhabwala, Z. Yu, S. Fan, Y. Avlasevich, K. Müllen, and W.E. Moerner. Large single-molecule fluorescence enhancements produced by a bowtie nanoantenna. *Nature Photon.*, 3:654–657, 2009.
- [74] T. Kosako, Y. Kadoya, and H.F. Hofmann. Directional control of light by a nanooptical Yagi-Uda antenna. *Nature Phot.*, doi:10.1038/nphoton.2010.34.
- [75] A.V. Krasheninnikov and F. Banhart. Engineering of nanostructures carbon materials with electron or ion beams. *Nature Mat.*, 6:723–733, 2007.
- [76] E. Kretschmann and H. Räter. Radiative decay of nonradiative surface plasmon excited by light. *Z. Natuf.*, 23A:2135–2136, 1968.
- [77] M.P. Kreuzer, R. Quidant, J.P. Salvador, M.P. Marco, and G. Badenes. Colloidal-based localized surface plasmon resonance (LSPR) biosensor for the quantitative determination of stanazol. *Anal. Bioanal. Chem.*, 391(5):1813–1820, 2008.
- [78] J. Ladd, A.D. Taylor, M. Piliarik, J. Homola, and S. Jiang. Label-free detection of cancer biomarker candidates using surface plasmon resonance imaging. *Anal. Bional. Chem.*, 393:1157–1163, 2009.
- [79] K.G. Lee, H.W. Kihm, J.E. Kihm, W.J. Choi and H. Kim, C. Ropers, D.J. Park, Y.C. Yoon, S.B. Choi, D.H. Woo, J. Kim, B. Lee, Q.H. Park, C. Lienau, and S. Kim. Vector field microscopic imaging of light. *Nature Phot.*, 1:53–56, 2007.
- [80] Z. Li, T. Shegai, G. Haran, and H. Xu. Multiple-particle nanoantennas for enormous enhancement and polarization control of light emission. *ACS Nano*, 3(3):637–642, 2009.
- [81] T.-J. Lin and M.-F. Chung. Detection of cadmium by a fiber-optic biosensor based on localized surface plasmon resonance. *Biosens. Bioelectron.*, 24(5):1213–1218, 2009.
- [82] N. Liu, L. Langguth, T. Weiss, J. Kästel, M. Fleischhauer, T. Pfau, and H. Giessen. Plasmonic analogue of electromagnetically induced transparency at the Drude damping limit. *Nature Mat.*, 8:758–762, 2009.
- [83] C. Loo, A. Lowery, N. Halas, J. West, and R. Drezek. Immunotargeted nanoshells for integrated cancer imaging and therapy. *Nano Lett.*, 5(4):709–711, 2005.

- [84] A. Madrazo and M. Nieto-Vesperinas. Scattering of electromagnetic waves from a cylinder in front of a conducting plane. *J. Opt. Soc. Am. A*, 12:1298–1309, 1995.
- [85] S.A. Maier, P.G. Kik, H.A. Atwater, S. Meltzer, E. Harel, B.E. Koel, and A. Requicha. Local detection of electromagnetic energy transport below the diffraction limit in metallic nanoparticle plasmon waveguides. *Nature Mat.*, 2:229–232, 2003.
- [86] V.P. Maltsev and V.N. Lopatin. Parametric solution of the inverse light-scattering problem for individual spherical particles. *Appl. Opt.*, 36(24):6102–6108, 1997.
- [87] J.M. Manceau, N.H. Shen, M. Kafesaki, C.M. Soukoulis, and S. Tzortzakis. Dynamic response of metamaterials in the terahertz regime: Blueshift tunability and broadband phase modulation. *Appl. Phys. Lett.*, 96:021111, 2010.
- [88] E. Marx and T.V. Vorburger. Direct and Inverse problems for light scattered by rough surfaces. *Appl. Opt.*, 29(5):3613–3626, 1990.
- [89] E. Matveeva, Z. Gryczynski, I. Gryczynski, J. Malicka, and J.R. Lakowicz. Myoglobin immunoassay utilizing directional surface plasmon-coupled emission. *Angew. Chem.*, 76:6287–6292, 2004.
- [90] J. C. Maxwell. *A Treatise on Electricity and Magnetism*. Clarendon Press, Oxford, 1873.
- [91] J.C. Maxwell. A dynamical theory of the electromagnetic field. *Philosophical Transactions of the Royal Society of London*, 155:459–512, 1865.
- [92] C. McDonagh, O. Stranik, R. Nooney, and B.D. MacCraith. Nanoparticles strategies for enhancing the sensitivity of fluorescence-based biochips. *Nanomedicine*, 4(6):645–656, 2009.
- [93] M. Meier and A. Wokaun. Enhanced fields on large metal particles: dynamic depolarization. *Opt. Letters*, 8(11):581–583, 1983.
- [94] O. Merchiers, F. Moreno, F. González, and J.M. Saiz. Light scattering by an ensemble of interacting dipolar particles with both electric and magnetic polarizabilities. *Phys. Rev. A*, 76(4):043834, 2007.
- [95] O. Merchiers, F. Moreno, F. González, J.M. Saiz, and G. Videen. Electromagnetic wave scattering from two interacting small spherical particles. influence of their optical constants, ϵ and μ . *Opt. Commun.*, 269(1):1–7, 2007.

- [96] H. Mertens, J. Verhoeven, A. Polman, and F.D. Tichelaar. Infrared surface plasmons in two-dimensional silver nanoparticle arrays in silicon. *Appl. Phys. Lett.*, 85(8):1317–1319, 2004.
- [97] G. Mie. Beiträge zur Optik trüber Medien, speziell kolloidaler Metallösungen. *Ann. Physik*, 25(4):377–445, 1908.
- [98] D.A.B. Miller. Are the optical transistors the logical next step? *Nature Phot.*, 4:3–5, 2010.
- [99] N.A. Mirin and N.J. Halas. Light-bending nanoparticles. *Nano Lett.*, 9(3):1255–1259, 2009.
- [100] J.J. Mock, M. Barbic, D.R. Smith, D.A. Schultz, and S. Schultz. Shape effects in plasmon resonance of individual colloidal silver nanoparticles. *J. Chem. Phys.*, 116(15):6755–6759, 2002.
- [101] P. Monk. *Finite elements methods for Maxwell's equations*. Oxford University Press, Oxford, USA, 2003.
- [102] F. Moreno, F. González, and J. M. Saiz. Plasmon spectroscopy of metallic nanoparticles above flat dielectric substrates. *Opt. Lett.*, 31(12):1902–1904, 2006.
- [103] F. Moreno, J.M. Saiz, P.J. Valle, and F. González. Metallic particle sizing on flat surfaces: Application to conducting substrates. *Appl. Phys. Lett.*, 68(22):3087–3089, 1996.
- [104] J.R. Mourant, J.P. Freyer, A.H. Hielscher, A.A. Eick, D. Shen, and T.M. Johnson. Mechanisms of light scattering from biological cells relevant to noninvasive optical-tissue diagnostics. *Appl. Opt.*, 37(16):3586–3593, 1998.
- [105] G. W. Mulholland, C. F. Bohren, and K. A. Fuller. Light Scattering by Agglomerates: Coupled Electric and Magnetic Dipole Method. *Langmuir*, 10:2533–2546, 1994.
- [106] J. Nelayah, M. Kociak, O. Stéphan, F. García de Abajo, M. Tencé, L. Henrard, D. Taverna, I. Pastoriza-Santos, L.M. Liz-Marzán, and C. Colliex. Mapping surface plasmons on a single metallic nanoparticle. *Nature Phys.*, 3:348–353, 2007.
- [107] P. Nordlander. Plasmon hybridization in nanoparticles near metallic surfaces. *Nano Lett.*, 4(11):2209–2213, 2004.

- [108] L. Novotny and B. Hecht. *Principles of Nano-Optics*. Cambridge University Press, Cambridge, 2006.
- [109] T. Okamoto and I. Yamaguchi. Optical absorption study of the surface plasmon resonance in gold nanoparticles immobilized onto a gold substrate by self-assembly technique. *J. Phys. Chem B*, 107(38):10321–10324, 2003.
- [110] P. Olk, J. Renger, M.T. Wenzel, and L.M. Eng. Distance dependent spectral tuning of two coupled metal nanoparticles. *Nano Lett.*, 8(4):1174–1178, 2008.
- [111] A. Otto. A new method for exciting nonradiative surface plasma oscillations. *Phys. Stat. Sol.*, 26:K99–K101, 1968.
- [112] R.A. Pala, J. White, E. Barnard, J. Liu, and M.L. Brongersma. Design of plasmonic thin-film solar cells with broadband absorption enhancements. *Adv. Mat.*, 21(34):3504–3509, 2009.
- [113] J. L. Peña, J.M. Saiz, and F. González. Profile of a fiber from backscattering measurements. *Opt. Lett.*, 25:1699–1701, 2000.
- [114] J.B. Pendry. Negative refraction makes a perfect lens. *Phys. Rev. Lett.*, 85:3966–3969, 2000.
- [115] J.B. Pendry, D. Schuring, and D.R. Smith. Controlling electromagnetic fields. *Science*, 312:1780–1782, 2006.
- [116] M. Piliarik, L. Párová, and J. Homola. High-throughput SPR sensor for food safety. *Biosensors and Bioelectronics*, 24(5):1399–1404, 2009.
- [117] R.G. Pinnick, S.C. Hill, P. Nachman, G. Videen, G. Chen, and R.K. Chang. Aerosol fluorescence spectrum analyzer for rapid measurement of single micrometer-sized airborne biological particles. *Aerosol Sci Technol.*, 28(12):95–104, 1998.
- [118] P. N. Prasad. *Nanophotonics*. John Wiley and Sons, New York, 2004.
- [119] Lord Rayleigh. On the transmission of light through an atmosphere containing small particles in suspension, and on the origin of the blue of the sky. *Philos. Mag.*, 47(287):375–384, 1899.
- [120] A.K. Sarychev and V.M. Shalaev. *Electrodynamics of metamaterials*. World Scientific, Singapore, 2007.

- [121] J.A. Schuller, E.S. Barnard, W. Cai, Y.C. Jun, J.S. White, and M.L. Brongersma. Plasmonics for extreme light concentration and manipulation. *Nature Mat.*, 9:193–204, 2010.
- [122] V.M. Shalaev. Optical negative-index metamaterial. *Nature Phot.*, 1:41–48, 2007.
- [123] V.M. Shalaev. Transforming light. *Science*, 322(5900):384–386, 2008.
- [124] T. Shegai, Y. Huang, H. Xu, and M. Käll. Coloring fluorescence emission with silver nanowires. *Appl. Phys. Lett.*, 96:103114, 2010.
- [125] L. Sherry, S.H. Chang, G. Schatz, and R. Van Duyne. Localized surface plasmons resonance spectroscopy of single silver nanocubes. *Nano Lett.*, 5:2034–2038, 2005.
- [126] M.G. Silveirinha, A. Alu, J. Li, and N. Engheta. Nanoinsulators and nanoconnectors for optical nanocircuits. *J. Appl. Phys.*, 103:064305, 2008.
- [127] S.B. Singham and C.F. Bohren. Light scattering by an arbitrary particle: a physical reformulation of the coupled dipole method. *Opt. Lett.*, 12(1):10–12, 1987.
- [128] D.R. Smith, J.B. Pendry, and M. C. Wiltshire. Metamaterials and negative refractive index. *Science*, 305:788–792, 2004.
- [129] D.R. Smith, S. Schultz, P. Markoš, and C.M. Soukoulis. Determination of effective permittivity and permeability of metamaterials from reflection and transmission coefficients. *Phys. Rev. B*, 65(19):195104, 2002.
- [130] S.D. Standridge, G.C. Schatz, and J.T. Hupp. Toward plasmonic solar cells: Protection of silver nanoparticles via atomic layer deposition of TiO_2 . *Langmuir*, 25(5):2596–2600, 2009.
- [131] P.L. Stiles, J.A. Dieringer, N.C. Shah, and R.P. Van Duyne. Surface-Enhanced Raman Spectroscopy. *Annu. Rev. Anal. Chem.*, 1:601–626, 2008.
- [132] K.H. Su, Q.-H. Wei, X. Zhang, J.J. Mock, D.R. Smith, and S. Schultz. Interparticle coupling effects on plasmons resonances of nanogold particles. *Nano Letts.*, 3(8):1087–1090, 2003.
- [133] Y. Sun and Y. Xia. Shape-controlled synthesis of gold and silver nanoparticles. *Science*, 298(5601):2176–2179, 2002.

- [134] J. Valentine, J. Li, T. Zentgraf, G. Bartal, and X. Zhang. An optical cloak made of dielectrics. *Nature Mat.*, 8:568–571, 2009.
- [135] J. Valentine, S. Zhang, T. Zentgraf, E. Ulin-Avila, D.A. Genov, G. Bartal, and X. Zhang. Three-dimensional optical metamaterial with a negative refractive index. *Nature*, 455:376–379, 2008.
- [136] P.J. Valle. *Sobre la interacción de ondas electromagnéticas con superficies constituidas por substratos planos y protuberancias de geometría cilíndrica. Aplicación del Teorema de Extinción*. PhD thesis, Universidad de Cantabria, Departamento de Física Aplicada, 1993.
- [137] P.J. Valle, F. González, and F. Moreno. Electromagnetic wave scattering from conducting cylindrical structures on flat substrates: study by means of the extinction theorem. *Appl. Opt.*, 33:512–523, 1994.
- [138] V. G. Veselago. The electrodynamics of substances with simultaneously negative values of ϵ and μ . *Phys. Usp.*, 10(4):509–514, 1968.
- [139] G. Videen and W. S. Bickel. Light-scattering resonances in small spheres. *Phys. Rev. A*, 45(8):6008–6012, 1990.
- [140] G. Videen, Y. Yatskiv, and M. Mishchenko. *Photopolarimetry in Remote Sensing*. Kluwer Academic Publishers, The Netherlands, 2004.
- [141] H. Wang, D.W. Brandi, P. Nordlander, and N.J. Halas. Plasmonic Nanostructures: Artificial Molecules. *Acc. Chem. Res.*, 40:53–62, 2007.
- [142] K. Wang, E. Schonbrun, and K. Crozier. Propulsion of gold nanoparticles with surface plasmon polaritons: Evidence of enhanced optical force from near-field coupling between gold particle and gold film. *Nano Lett.*, 9(7):2623–2629, 2009.
- [143] R. Weissleder and V. Ntziachristos. Shedding light onto live molecular targets. *Nature Med.*, 9:123–128, 2003.
- [144] W. Yan, X. Feng, X. Chen, W. Hou, and J.-J. Zhu. A super highly sensitive glucose biosensor based on Au nanoparticles-AgCl@polyaniline hybrid material. *Biosens. Bioelectron.*, 23:925–931, 2008.

- [145] X. Wei, X. Luo, X. Dong, and C. Du. Localized surface plasmon nanolithography with ultrahigh resolution. *Opt. Express*, 15:14177–14183, 2007.
- [146] Y. Yanase, A. Araki, H. Suzuki, T. Tsutsui, T. Kimura, K. Okamoto, T. Nakatani, T. Hiragun, and M. Hide. Development of an optical fiber SPR sensor for living cell activation. *Biosens. Bioelectron.*, 25(5):1244–1247, 2010.
- [147] R.J. Zemp. Detecting rare cancer cells. *Nature Nanotech.*, 4(12):798–799, 2009.
- [148] N.I. Zheludev. The road ahead for metamaterials. *Science*, 328:582–583, 2010.
- [149] J. Zhu and Y. Cui. Photovoltaics: more solar cells for less. *Nature Mat.*, 9:183–184, 2010.
- [150] R. Zhu, J. Wang, and G. Jin. Mie scattering calculation by FDTD employing a modified Debye model for gold material. *Optik-Intern. J. Light and Elec. Opt.*, 116:419–422, 2005.

